BOREAL ENVIRONMENT RESEARCH 30: 221–241
ISSN 1797-2469 (online)

Helsinki 19 December 2025

Intervention of pollution episodes from nearby sawmills to ecosystem-atmosphere interactions studied in a boreal forest at SMEAR II

Ilona Ylivinkka[1)2)*], Carla Di Natale[3)], Marie K. Mikkelsen[4)], Aki Nissinen[5)], Luisa Pennacchio[4)], Jani Strömberg[1)], Olli Saranko[3)], Laura Utriainen[3)], Rafael Valiati[6)], Juho Aalto[7)], Sujai Banerji[1)], Liine Heikkinen[8)9)], Anna Lintunen[1)], Krista Luoma[3)], Otso Peräkylä[1)], Nina Sarnela[1)], Ditte Taipale[1)], Risto Taipale[1)2)], Steven J. Thomas[1)], Xinran Zhang[1)] and Markku Kulmala[1)]

[1)] *Institute for Atmospheric and Earth System Research / Physics, Faculty of Science, University of Helsinki, P.O. Box 64, 00014 Helsinki, Finland*
[2)] *SMEAR II station, University of Helsinki, Hyytiäläntie 124, 00014 University of Helsinki, Finland*
[3)] *Finnish Meteorological Institute, Erik Palménin aukio 1, 00560 Helsinki, Finland*
[4)] *Department of Chemistry, University of Copenhagen, Universitetsparken 5, 2100 Copenhagen, Denmark*
[5)] *Department of Technical Physics, University of Eastern Finland, Yliopistonranta 8, 70211 Kuopio, Finland*
[6)] *Department of Applied Physics, Physics Institute, University of São Paulo, São Paulo, Brazil*
[7)] *Hyytiälä Forest Station, Faculty of Agriculture and Forestry, University of Helsinki, Hyytiäläntie 124, 00014 University of Helsinki, Finland*
[8)] *Department of Environmental Science, Stockholm University, 11418 Stockholm, Sweden*
[9)] *Bolin Centre for Climate Research, Stockholm University, 11418 Stockholm, Sweden*
**corresponding author's e-mail: ilona.ylivinkka@helsinki.fi*

Received 19 Sep. 2025, final version received 13 Nov. 2025, accepted 21 Nov. 2025

Ylivinkka I., Natale C.D., Mikkelsen M.K.,Nissinen A., Pennacchio L., Strömber J., Saranko O., Utriainen L., Valiati R., Aalto J., Banerji S., Heikkinen L., Lintunen A., Luoma K., Peräkylä O., Sarnela N., Taipale D., Taipale R., Thomas S.J., Zhang X. & Kulmala M. 2025: Intervention of pollution episodes from nearby sawmills to ecosystem-atmosphere interactions studied in a boreal forest at SMEAR II. *Boreal Env. Res.* 30: 221–241.

Some atmospheric compounds are emitted by both natural and anthropogenic sources, making them hard to distinguish. For instance, sawmills emit large amounts of volatile organic compounds, which are released from wood in different processing stages. SMEAR II (Station for Measuring Ecosystem–Atmosphere Relations) is located near sawmills in Korkeakoski (6 km southeast from SMEAR II) and Vilppula (21 km northeast from SMEAR II). Long-term measurements show that monoterpene concentrations were more than three times higher when the wind was from the Korkeakoski direction. Concentrations of NO_x, O_3, and Aitken mode-sized particles were also impacted by the sawmills. Perturbations were less clear from the Vilppula direction, likely because it was less frequent wind direction, and the transport distance was longer. We recommend considering the influence of the sawmills on the above-mentioned variables in future analyses of biosphere–atmosphere interactions, to avoid a distinct anthropogenic influence from the nearest sawmills.

Editor in charge of this article: Antti Arola
https://doi.org/10.60910/ber2025.727e-sw95

Introduction

Atmospheric composition is modulated by natural and anthropogenic emission sources, either emitted locally or transported over long distances. The separation between natural and anthropogenic sources is often challenging since many compounds have both natural and anthropogenic sources. One such example is sawmills producing sawn timber. High concentrations of volatile organic compounds (VOCs) have been measured near sawmills (Ingram *et al.* 1995, Broege *et al.* 1996, Granström 2007). Especially monoterpenes, which are a group of isomeric compounds, are emitted from sawmills processing spruce and pine (Ingram *et al.* 1995, Broege *et al.* 1996, Granström 2007, Liao *et al.* 2011). Although these emissions are caused by anthropogenic activities, the emissions as such are of biogenic origin and therefore contain many similar features as high concentrations of biogenic emissions (Rinne *et al.* 2009, Hellén *et al.* 2018). The concentrations related to sawmill emissions, however, can exceed the natural background levels by 10 to 1000 times (Granström 2007, Liao *et al.* 2011).

The emissions of VOCs near sawmills are caused by stocks of logs, sawdust, chips, and sawn timber stored at sawmills, since VOCs gradually evaporate from special storage structures, such as resin ducts (Grote and Niinemets 2008, Ghirardo *et al.* 2010). Further, when producing sawn timber, wood is dried in kilns, which has been shown to release up to 50% of the original VOC content of trees (Ingram *et al.* 1995, Englund and Nussbaum 2000). For spruce and pine, the most commonly emitted compounds in kiln drying are monoterpenes, contributing more than 90% of the total emissions by mass, but also emissions of acetic acid, formic acid and formaldehyde have been detected (Ingram *et al.* 1995, Broege *et al.* 1996).

SMEAR II (Station for Measuring Earth surface–Atmosphere Relations) in southern Finland is a rural background measurement site with a focal point of research to assess interactions between various processes in ecosystems and atmosphere (Hari and Kulmala 2005, Neefjes *et al.* 2022). Earlier studies have, for example, discovered mechanisms how oxidation products of VOCs originating from the surrounding boreal forest can contribute to formation and growth of aerosol particles (e.g., Tunved *et al.* 2006, Peräkylä *et al.* 2014, Mohr *et al.* 2019). Particles further impact the radiative balance of the Earth by acting as cloud condensation nuclei, thus modulating cloud properties (Kerminen *et al.* 2012, Yli-Juuti *et al.* 2021, Artaxo *et al.* 2022). They thereby also enhance both ecosystem and branch level photosynthesis by increasing the diffuse fraction of global radiation (Ezhova *et al.* 2018, Neimane-Šroma *et al.* 2024).

Occasionally, enhanced monoterpene concentrations have been measured at SMEAR II, which have been connected to activities at two sawmills located next to each other in Korkeakoski, 6 km southeast from the station (Liao *et al.* 2011, Williams *et al.* 2011, Hellén *et al.* 2018, Liebmann *et al.* 2018). Furthermore, Hakola *et al.* (2012) connected a fraction of the elevated concentrations also to a sawmill in Vilppula, 21 km northeast from the station. Due to the oxidation of monoterpenes, also increased particle number and organic aerosol concentrations have been measured when the sampled air masses originated from the Korkeakoski sawmill direction (Eerdekens *et al.* 2009, Liao *et al.* 2011, Heikkinen *et al.* 2020). Further, Pospisilova *et al.* (2020) showed in a chamber study that the secondary organic aerosol (SOA) composition formed from the sawmill emissions at SMEAR II was very similar to aerosol formed in ozonolysis of alpha-pinene, which is a dominant monoterpene at SMEAR II (Bäck *et al.* 2012, Hakola *et al.* 2012, Hellen *et al.* 2018). Hence, as the emissions from sawmills constitute of the same compounds as emitted from the surrounding forest, it is difficult, but crucial, to distinguish the sources rigorously when investigating ecosystem–atmosphere relationships.

Sawmill activities can also lead to emissions of other anthropogenic pollutants, such as soot, CO and NO_x due to machinery operations (Adhikari and Ozarska 2018). These emissions, as well as other released compounds, affect atmospheric composition and chemistry. Therefore, in order to best assess the naturally occurring atmosphere–biosphere interactions, the influence of the sawmills needs to be well accounted for.

In the study by Eerdekens *et al.* (2009), the sawmill influence was detected due to conspicuously strong nighttime particle formation event with simultaneous increase in monoterpene concentrations during a measurement campaign in April 2005. In Liao *et al.* (2011), in turn, the pollution episodes were detected based on anomalously high monoterpene concentrations, using data from 580 days between June 2006 and March 2009. Here, we distinguish data influenced by sawmill activities based on wind direction and air mass back trajectories, enabling us to assess the impacts of sawmill emissions on atmospheric composition, and use long-term dataset from January 2011 to December 2023 to quantify sawmill influence on various parameters. Moreover, we investigate in detail the impacts of the sawmill further away in Vilppula. With this approach and long-term measurements, we can more precisely identify and quantify how the atmospheric variables are affected by the sawmill industry.

Material and methods

Site description

SMEAR II (61°51′N, 24°17′E; 181 m a.s.l.) is located in southern Finland and is surrounded by 63-years-old, Scots pine (*Pinus sylvestris*) dominated forest (Hari and Kulmala 2005), with a current mean canopy height of about 20 m. The nearest large city is Tampere with 255 000 inhabitants, located about 50 km southwest from the station. UPM Korkeakoski and JPJ-Wood sawmills are located next to each other in Korkeakoski, about 6 km southeast from SMEAR II. UPM Korkeakoski produces sawn timber from pine with a yearly production capacity of 350 000 m^3 (UPM 2025a) and JPJ-Wood from spruce and pine with a yearly production capacity of 200 000 m^3 (JPJ 2025). Metsä Fibre sawmill is located in Vilppula, about 21 km northeast from SMEAR II, producing mainly sawn spruce timber with a yearly production of 535 000 m^3 (Metsä Group 2024). The roundwood consumption at Finnish sawmills is about 2.1 times higher compared to the produced timber, the number growing to 2.7 when accounting also the volume of bark (UNECE 2010), hence significantly increasing the total amount of wood stored and processed at sawmills.

Measurement description

In this work, we use data from 2011 to 2023 to quantify the effects of the sawmill activities on the atmospheric observations at SMEAR II. In early 2020, the forest around the SMEAR II station was thinned, which is a common procedure in managed forests of Finland. About 40% of the tree basal area was removed to make more space for the remaining trees to grow larger in size (Aslan *et al.* 2024). Due to the thinning, a period spanning from February to June 2020 was removed from the analysis, as forest felling induces significant emissions of monoterpenes for several weeks to months (Räisänen *et al.* 2008, Haapanala *et al.* 2012), and hence the period does not represent the typical conditions at the site.

VOC measurements

At SMEAR II, VOCs are continuously monitored with Proton-Transfer-Reaction Quadrupole Mass Spectrometer (PTR-QMS, Ionicon). The instrument measures concentrations of 12 compounds identified using mass-to-charge ratios (*m/z*) in unit mass resolution. PTR-QMS measures ambient concentrations for one hour every three hours from eight heights (4.2, 8.4, 16.8, 33.6, 50.4, 67.2, 101, and 125 m), with up to nine scans per height. This study uses data collected from the 67.2 m level, to be clear of the canopy. Some compounds have the same *m/z*, making them indistinguishable from each other. These include formic acid+ethanol, isoprene+methylbutenol fragment (MBO), methacrolein+methyl vinyl ketone (MVK), and toluene+p-cymene fragment (hereon called toluene+p-cymene). Other analyzed VOCs are methanol, acetonitrile, acetaldehyde, acetone, acetic acid, methyl ethyl ketone (MEK), benzene, and sum of monoterpenes (MTs). The instrument is calibrated frequently using the procedure described in Taipale *et al.* (2008).

Greenhouse and trace gas measurements

We also analyzed the greenhouse gases, carbon dioxide (CO_2) and methane (CH_4), both of which have long atmospheric lifetimes, ranging from ten to hundreds of years. In addition, we analyzed the trace gases carbon monoxide (CO), nitric oxide (NO), nitrogen oxides (NO_x), ozone (O_3), and sulfur dioxide (SO_2). SO_2 has a lifetime of hours to days, and CO of weeks to months (Hellén *et al.* 2004, Wallace and Hobbs 2006, Riuttanen *et al.* 2013). NO, NO_x and O_3 are cycled photochemically, with especially O_3 being a secondary pollutant, formed through atmospheric chemistry (Wallace and Hobbs 2006). The concentrations were measured at 67.2 m height except for the concentration of SO_2, which is an average of all eight measurement heights because of its low atmospheric concentration at SMEAR II. Trace gases were recorded every 6 min. The measurement frequency for CO_2 was every 6 minutes until 2017 after which, it was recorded every 30 minutes due to instrumental changes. The measurement for CH_4 occurred every 30 minutes throughout the study period (2011–2023). CO was measured with infrared light absorption analyzers APMA 370 (Horiba) until February 2016 and afterwards with API 300EU (Teledyne). O_3 was measured with a TEI 49 C (Thermo Scientific) ultraviolet light absorption analyzer, NO and NO_x with a TEI 42iTL (Thermo Scientific) chemiluminescence analyzer and SO_2 with a TEI 43i-TLE (Thermo Scientific) fluorescence analyzer. Until end of 2017 CO_2 was measured with LI840 (LI-COR) infrared gas analyzer and after that with G2401 (Picarro) cavity ring-down spectrometer (CRDS) as a part of the Integrated Carbon Observation System (ICOS). CH_4 was measured with a G1301 (Picarro) CRDS between February 2012 and October 2014 and since then with G2401 (Picarro).

Highly oxygenated organic molecule measurements

Highly oxygenated organic molecules (HOM) are formed in the atmosphere via autoxidation involving peroxy radicals arising from oxidation of certain VOCs, such as monoterpenes (Bianchi *et al.* 2019), and are used here to represent oxidation products of VOCs emitted from the sawmills. HOMs are measured using the Chemical Ionization Atmospheric Pressure interface Time-Of-Flight (CI-APi-TOF) mass spectrometer (Jokinen *et al.* 2012). HOM consist of both monomers (here sum of *m/z* 290–430) and dimers (sum of *m/z* 430–620). HOMs are measured at the height of 35 m, and the data is available from 2016 to 2023, except for 2020 and 2021 due to instrument failure. From 2016 to 2017 HOM measurements are averaged every 10 minutes, while from 2018 to 2023 every 30 minutes. It is worth noting that, following the maintenance of the instrument in the summer of 2022, there has been a noticeable decrease in the estimated HOM concentrations compared to previous measurements (2016–2019), indicating a potential change in instrument transmission, and other changes in the sensitivity are also possible. Hence, data from 2016–2019 and 2022–2023 are treated separately in the analysis.

Aerosol measurements

Aerosol particles are measured at ground level (4 m height) at SMEAR II with multiple instruments in order to describe the physicochemical properties of the particles. A Differential Mobility Particle Sizer (DMPS) is used for measuring the size distributions of fine aerosols in the 3–1000 nm range in 10 min time resolution (Aalto *et al.* 2001) and a Neutral Cluster and Air Ion Spectrometer (NAIS; Airel; Mirme & Mirme 2013) of ions from 0.8 to 42 nm and size distribution of aerosol particles from 2 to 42 nm in 1 min time resolution. In this work, we utilized only negative ion concentration from 2 to 7 nm from NAIS to understand the local effect on aerosol growth (Tuovinen *et al.* 2024) as well as aerosol size distribution data from DMPS.

The mass concentration of sub-micrometer organic aerosol (OA) was retrieved from Aerosol Chemical Speciation Monitor (ACSM; Aerodyne Research) with 30 min time resolution (Heikkinen *et al.*, 2020).

Finally, a TSI 3563 Integrating Nephelometer, was used to estimate radiation scattering

coefficient (σ_{sca}) at multiple wavelengths (450, 550, and 700 nm), and a AE31 until 2018 and after that AE33 (Aerosol Magee Scientific) aethalometer, estimating absorption coefficient (σ_{abs}) of aerosols at seven wavelengths (370, 470, 520, 590, 660, 880, and 950 nm). The AE31 and AE33 measurements are converted to equivalent black carbon (eBC) concentrations at 880 nm (Hyvärinen *et al.* 2011). To correct for the so-called filter-loading effect, the AE31 data are corrected by an algorithm by Virkkula *et al.* (2007) and using a multiple scattering correction factor of 3.14 derived by Luoma *et al.* (2021), whereas the AE33 applies an inbuilt correction (Drinovec *et al.* 2015). To convert from σ_{abs} to eBC, mass absorption cross section values of 4.78 m^2 g^{-1} for AE31 data (derived from 6.6 m^2 g^{-1} at 637 nm used for multi-angle absorption photometer) and 7.77 m^2 g^{-1} for AE33 data (according to instrument manual) at 880 nm are used. The optical data are available in hourly averages.

The optical properties of aerosols were also used for calculating Single Scattering Albedo (SSA):

$$SSA_{\lambda} = \frac{\sigma_{scat,\lambda}}{\sigma_{abs,\lambda} + \sigma_{scat,\lambda}} \quad (1)$$

(Seinfeld and Pandis 2012). $\sigma_{scat,\lambda}$ and $\sigma_{abs,\lambda}$ in Eq. 1 represent the scattering and absorption coefficients, respectively, estimated for the same wavelength, which was defined as 550 nm as it is representative of the visible spectrum. Due to the mismatch of wavelengths in the utilized instruments, the absorption coefficient Ångström exponent-based interpolation was implemented for this calculation. The SSA is a dimensionless intrinsic property of the aerosol population, meaning that it does not depend on concentrations, which leads to variations representing fundamental changes in the properties of such particles.

Air mass back trajectories

The HYSPLIT (Hybrid Single Particle Lagrangian Integrated Trajectory) model is used to compute dispersion and trajectories of air masses. The model was developed at NOAA's (National Oceanic and Atmospheric Administration) Air Resources Laboratory. The model uses both Lagrangian approach and Eulerian approach as the methods of calculation (Stein *et al.* 2015). In this study, the backward mode of the HYSPLIT-WEB was used to determine the origins of air masses reaching SMEAR II during the studied days. Reanalysis data from the National Centers for Environmental Prediction (NCEP) and the National Center for Atmospheric Research (NCAR) at a 2.5-degree spatial resolution was used as the meteorological data for the model simulations. The length of the model runs varied between the studied days. The closest point between the trajectories and the sawmills was estimated by linearly interpolating between the time steps. In addition, diagnostic mixing layer height from HYSPLIT simulations was used to determine whether the air masses passed the sawmills in the mixed layer and, thus, contained air that could have been influenced by the sawmills. Lastly, the trajectories were flagged as a possible sawmill episode if the interpolated lines passed within a 1 km radius centered at the sawmills. As the spatial resolution of the used meteorological data is very coarse compared to the distances between the sawmills and the station, the air mass back trajectories are used only as an ancillary study method. For this same reason, it is not necessary to calculate air mass trajectories for the different measurement heights of SMEAR II, but only at the heights corresponding to the wind direction measurements. Further, the measurements are generally conducted within boundary layer (Sinclair *et al.* 2022), and hence the variation in concentration between different measurement heights is rather small (Zha *et al.* 2018, Lampilahti *et al.* 2021).

Sawmill episode identification

Sawmill episodes were identified using wind direction data measured at 67.2 m and 33.6 m altitude above the ground level. Days were flagged if either measurement height showed prevailing winds coming from the sawmills. In order to get a clean baseline, the flagging for background days required both heights to show prevailing wind from the background sector. The two heights were chosen as they both had good

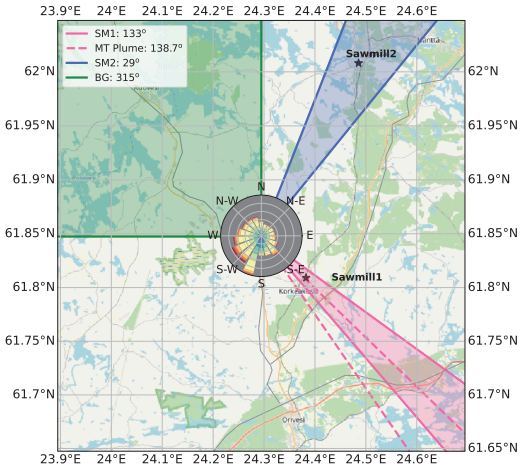

Fig 1. SMEAR II measurement site location relative to the sawmill and background wind sectors. The location of the center of each sector is shown in the legend and width of each sector is indicated with a shaded area. A wind rose showing the prevailing wind directions from 67.2 m height at the site between years 2011 and 2023 is added to the figure. An additional sector towards SM1 is plotted with dashed lines to show the difference in direction between the compass direction and a visible MT plume.

data availability (over 90% in 2011–2023) and were measured above the canopy level, which decreases the effect of surface roughness elements on wind speed and direction (Rannik *et al.* 2004). The main interest in terms of wind direction was whether there exists a possible signal from the nearby sawmills or not. These sawmill sectors are from here onwards referred to as Sawmill 1 (SM1) for the UPM Korkeakoski and JPJ-Wood sawmills (UPM 2025a, JPJ 2025), and Sawmill 2 (SM2) for the Metsä Fibre sawmill (Metsä Group 2024). Furthermore, a background (BG) sector towards the northwest was chosen to get a clean baseline to compare against the sawmill sectors (Fig. 1). The effect of nearby populated areas, such as Tampere (215°), was taken into account when choosing the width and direction of the background sector.

To ensure sufficient periods with prevailing wind directions from the chosen sectors and the low time resolution of VOC measurements, we categorized each day of the measurement period by the selected sectors. The SM1 sector size was chosen to be 10°, due to it being both sufficiently large to cover both sawmills and because it captured most of the MT plume coming from this sector (see Sect. 3.1). The SM2 sector size was increased to 20° due to the larger distance between the sawmill and the measurement site. For SM1 and SM2, at least 25% of the daily data points were required to originate from the specified sector in order to flag the day as a potential sawmill episode, while BG had a stricter 90% criterion for a day to be flagged as a BG day. This approach aimed to secure an ample number of clean baseline days while minimizing the impact of other wind directions. Using this classification, 842 days satisfying one of the three thresholds for wind directions were found. The overall distribution and details of each sawmill episode category are presented in Table 1. Color coding is used in all figures to differentiate between the sectors. Figure 1 also shows the discrepancy between the actual direction of SM1 (solid lines) and the observed MT plume coming from the SM1 direction (dashed lines). This offset is +5.7° and is further explained in Sect. 3.1. All results and data analysis from hereon for SM1 has been done using the sector aligned with the MT plume.

Method description

The difference in studied variables between the sectors was investigated through notched boxplots and density plots. All data points divided into the selected sectors were used, except for the VOCs, where the 24-hour (daily) medians were used due to the low measuring frequency. For the

Table 1. Table of the wind sector flagging, showing the compass direction of the sector's center, width of each sector, threshold for daily percentage of data points originating in the sector to flag the day as sawmill episode day, and the total number of flagged sawmill episode days per sector between 2011 and 2023. BG is the background sector, and SM1 and SM2 refer to the Korkeakoski and Vilppula sawmill sectors, respectively.

	Direction	Sector width	Threshold	No. of days
BG	315.0°	90°	90%	400
SM1	138.7°	10°	25%	177
SM2	29.0°	20°	25%	265

shown boxplots, median value is represented by a black line, and the mean value as a black diamond. The notches show an approximate 95% confidence interval around the median. As is commonly done with notched boxplots, we take non-overlapping notches between two groups as a visual indication that their medians differ significantly. The box encloses the interquartile range (IQR), which represents the middle 50% of the data, from 25th to 75th percentiles. The whiskers extend from the 10th to the 90th percentiles. Data points outside of this range are considered outliers and are represented by black circles. They are excluded from the visualization of the greenhouse and trace gas boxplots due to the high amount of data points, resulting in a high number of outliers that lowered the clarity of the boxplots.

Potential correlations between the concentrations of HOMs, MTs, and O_3 were investigated for the sawmill sectors. Hourly median of HOMs and O_3 concentrations were computed to have consistent datasets to compare with MTs. As addressed in Sect. 2.2.3, the HOM concentrations are lower for the years 2022 and 2023 compared to previous years, because of possible changes in the instrument transmission. Therefore, in the scatter plots, the data from 2016 to 2019 are distinguished from the data from 2022 to 2023 by using different markers. Additionally, Pearson's correlation coefficient was computed separately for all available years (2016–2023), and for the years before the major maintenance (2016–2019) to better represent the overall HOM concentrations at SMEAR II and to exclude the influence of the data with lower concentration values.

In order to investigate the same question, but from a different point of view, the ratio between HOMs and MTs was computed to check for possible correlations between this ratio and O_3. The distinction between the two groups of data (2016–2019, and 2022–2023) was performed by using different colors. The same approach was adopted to investigate potential correlations between HOMs and negative ions.

When analyzing the effects of sawmills on the aerosol number size distribution, the data was filtered based on new particle formation (NPF) event classification to make sure differences in the data were not due to pervious days' NPF event. The classification divides each day either to NPF event (with three subcategories Ia, Ib, and II), non-event, undefined, partly bad data, or bad data day as described in Dal Maso *et al.* (2005). For a day to be included in the size distribution analysis, it needed to be a non-event day and follow a non-event day.

Results and discussion

Monoterpene-rich plume

A polar plot of measured MT concentrations by wind speed and direction showed a significant increase in concentration when wind roughly originated from the direction of SM1 (Fig. 2a). The magnitude of this increase suggested a presence of a large anthropogenic source near the station, considering the relative homogeneity of the forest around SMEAR II. Hourly averaged MT concentration as a function of wind direction, along with a least-squares fitted Gaussian distribution, consistent with the most commonly applied plume dispersion models (Snoun *et al.* 2023), are shown in Fig. 2b. The fitted peak center is located at 138.7°±0.2°, with a standard deviation of 5.7°±0.2°, with good agreement between the data and the fitted function. As explained in Sect. 2.3, the compass direction from Hyytiälä to SM1 is in fact 133°, meaning that there was a 5.7° difference between the sawmill's actual direction and the direction at which the monoterpene signal was observed. The difference likely came from a slight misalignment of the anemometer at SMEAR II after an instrument replacement in November 2015, since Liao *et al.* (2011) did not observe discrepancy between the center of the MT plume and the SM1 direction in their previous work. Moreover, applying the Gaussian fitting method for the MTs and wind direction data before 2015, the peak center located at 133.9°, which further verified the hypothesis of anemometer misalignment in the recent years.

If including only data prior to 2015 to the analysis, the MT plume from SM1 had a much smaller difference to the average background concentration compared to the data after 2015.

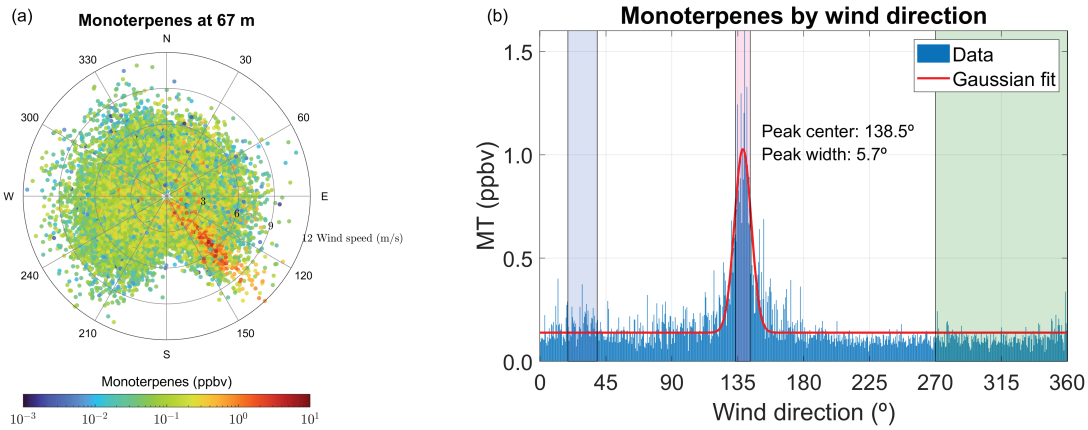

Fig 2. (**a**) Polar plot of all available MT concentration data by wind speed and direction, in hourly averages. Note that the color scale is logarithmic. See the wind rose on Fig. 1 to assess the occurrence likelihoods of the different wind speed and direction combinations. (**b**) Hourly averaged MT concentration as a function of wind direction at 0.5° steps. The red line shows a Gaussian function fitted to the data and the shaded areas mark the different wind sectors (SM1 in red, SM2 blue, and the BG sector in green color).

The intensity change suggests that there has been an enrichment of MT emissions from SM1, which could be explained by increased production capacity of the sawmills and indeed, since 2015 the annual production capacity of JPJ-Wood has increased from about 100 000 m^3 to 200 000 m^3 and UPM Korkeakoski's from 330 000 m^3 to 350 000 m^3 (UPM 2016, 2025a, JPJ 2025).

Based on the fitting parameters, a 10° sector centered at the direction defined by the Gaussian peak center, fitted using all available data, was designated to represent the SM1 for the remainder of this study. Considering the peak width of 5.7°, a 10° sector represents approximately a window of 1 standard deviation around the peak center, which encompasses the majority of the MT-enriched measurements, restricting the sector to avoid the inclusion of weaker events. Furthermore, increase in MT concentration from the SM2 sector was minor compared to the SM1 sector.

Wind conditions at SMEAR II

Wind conditions in Finland are mostly dominated by the mid-latitude synoptic scale low pressure systems, with the prevailing wind direction being southwest (Gregow *et al.* 2020). The seasonal distribution of wind direction and speed at SMEAR II is presented as wind roses in Fig. 3. The most prominent wind direction was confirmed to be southwest, but with a larger fraction of southeasterly winds during wintertime (Fig. 3). The general direction of the SM2 can also be observed to be among the rarest of wind directions throughout all seasons, which combined with a longer distance from the measurement site, means that an overall stronger effect of SM1 is to be expected.

Higher concentrations of MTs were generally measured at SMEAR II when the wind came from the SM1 sector, especially in autumn and winter, when nearly 20% of the total measured MT signal were associated with SM1 winds, while only 4% of the winds actually came from this small 10° sector (Fig. 4).

Mean wind speeds on SM1 episode days were on average 1.2 times higher compared to SM2 days, with an increase from 3.8 to 4.7 m s^{-1} (see Fig. S1 in Supplementary Information). Due to the differences in mean wind speeds and the overall distances from the sawmills to the measurement site, signals from the SM1 are expected to reach SMEAR II on average after 21 min, whereas the travel time increases to 91 min for possible SM2 signals. Also, the SM1 influence was more common during winter when the natural sources of MTs are negligible due to cold temperatures and little photosynthetic activity (e.g., Aalto *et al.* 2015), whereas SM2 influence

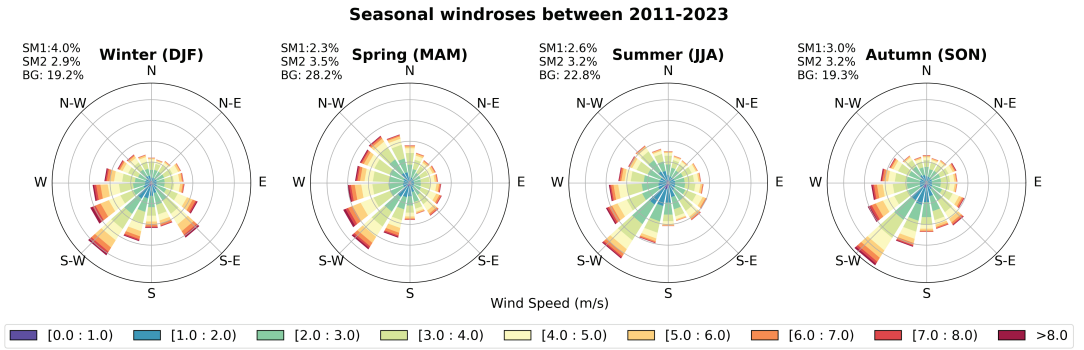

Fig 3. The average seasonal distribution of wind speed and direction as wind roses. The color bar shows the wind speed in ms^{-1}. The fractions of winds coming from each sector specified in Table 1 are shown in the top left corner for each wind rose.

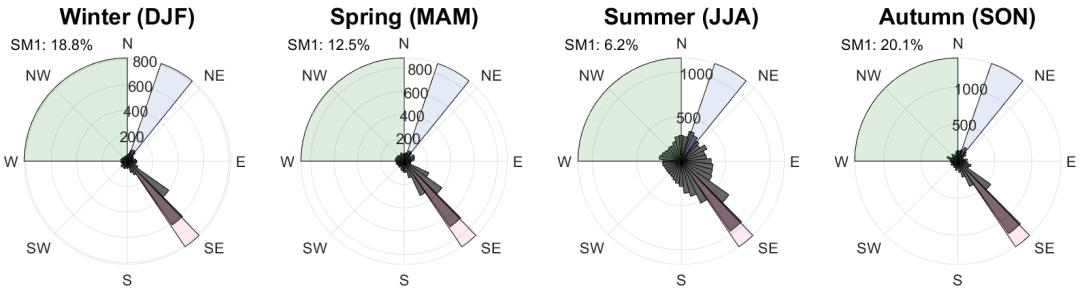

Fig 4. Average concentration of MTs (dark gray color) grouped by wind direction in each season. The SM1 sector is indicated with red color, SM2 with blue, and the BG sector with green color. The radial axis is the mean MT concentration in ppb. In each plot, the percentage of the total measured MT signal associated with SM1 winds is also shown.

was more evenly distributed throughout the year (see Fig. S2 in Supplementary Information).

VOC concentration dynamics

Due to the low time resolution of VOC measurements, we made boxplots of daily median concentrations, separated into BG, SM1, and SM2 days (Fig. 5). The dataset from 2011 to 2023 had many periods of missing VOC concentration data, lowering the overlap with the sawmill episode days. Compared to the BG days, the notched boxplots indicate that SM1 days had statistically significantly higher concentrations of MTs, isoprene+MBO, acetaldehyde, methacrolein+MVK, and MEK, which have mostly biogenic sources, but also benzene and toluene+p-cymene, which are commonly associated with anthropogenic pollution (Kansal 2009). The difference for the SM1 and SM2 days compared to the BG days can be seen in Table 2. On SM1 days, the concentration of MTs, benzene, and toluene+p-cymene were more than three times higher compared to the BG concentrations, with MTs showing the largest increase (3.3 times higher). Out of these VOCs, MEK showed the smallest increase (1.6 times higher) for the SM1 sector. Compared to all other wind directions, the SM1 sector showed 2.6 times higher MT concentration, which highlights the regional significance of MTs from the SM1 sector to the measured MT concentrations at SMEAR II.

The SM2 days had a smaller, but statistically significant increases in MTs, MEK, benzene, and toluene+p-cymene concentrations, as compared to the BG. The highest increase was, in this case, observed for toluene+p-cymene (1.4 times higher), whereas MEK, again, showed the smallest increase (1.2 times higher). However, comparing the increases between the SM1 and SM2 days, it is clear that the SM1 sector has a stronger

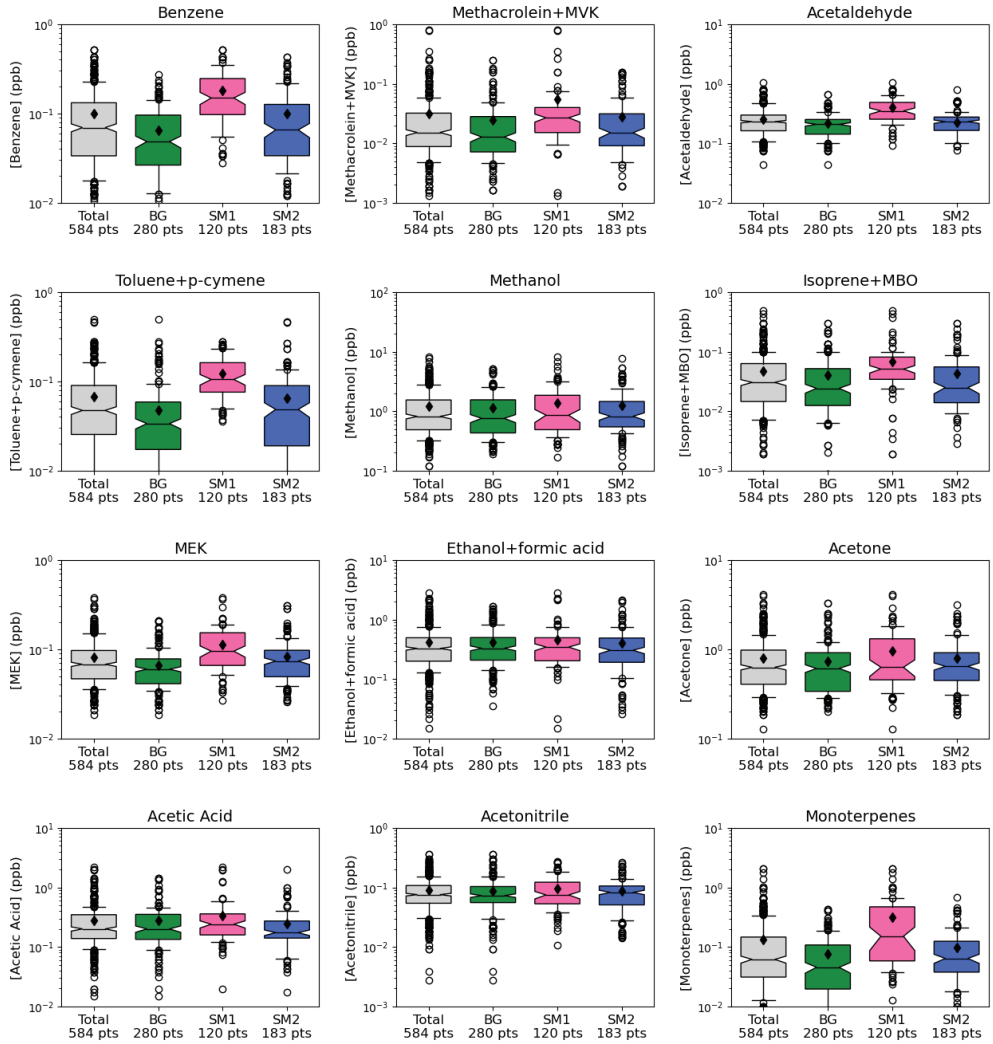

Fig 5. Boxplots of daily median VOC concentrations separated into BG, SM1, and SM2 days, gray marking the daily median of all groups. The median is shown with a black line, the mean value with a black diamond point, and outliers with black circles. The box edges extend to 25th and 75th percentiles while whiskers display the 10th and 90th percentiles. Overlapping notches indicate that the medians do not differ statistically significantly in 95% confidence level. The number of data points (equal to the number of days) is shown below the plots.

Table 2. Difference in the median concentration of individual VOCs between SM1 and BGs days, and SM2 and BG days, respectively. The difference is expressed in ppt and as a factor showing how much higher the concentrations during sawmill episode days are compared to the BG days.

VOC	Δ_{SM1} (ppt)	Δ_{SM1} (factor)	Δ_{SM2} (ppt)	Δ_{SM2} (factor)
Monoterpenes	106	3.32	19	1.41
Acetaldehyde	141	1.68	23	1.11
Methacrolein+MVK	14	2.10	2	1.18
Benzene	101	3.08	17	1.35
Toluene+p-cymene	71	3.12	15	1.44
Isoprene+MBO	27	2.11	1	1.03
MEK	35	1.59	14	1.23

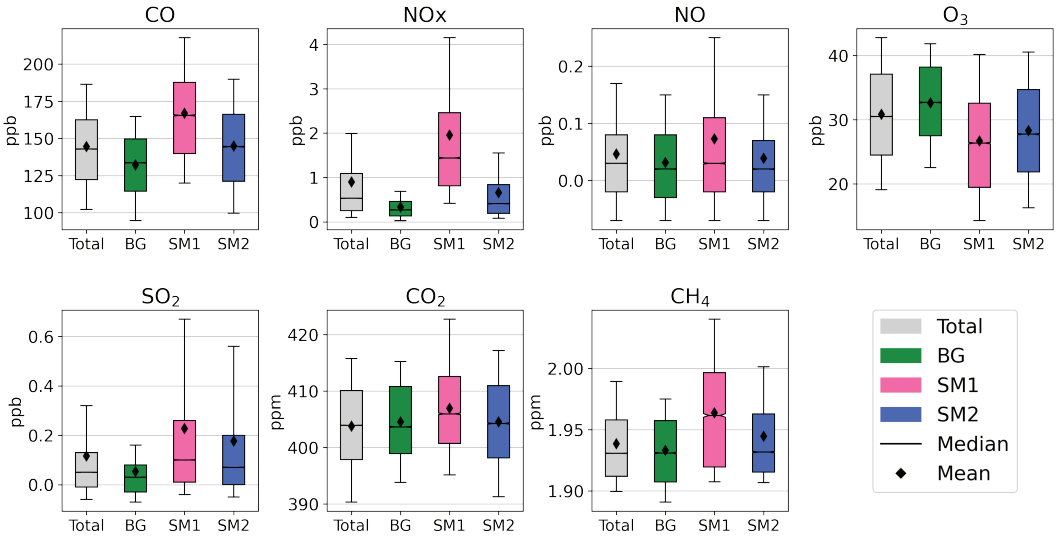

Fig 6. Boxplot of CO, NO_x, NO, O_3, SO_2, CO_2, and CH_4 concentrations in original time resolution separated into BG, SM1, and SM2 sectors, gray marking combination of all groups. Markers as in Fig. 5. The number of data points is presented in Table S2 in Supplementary Information.

influence on VOC concentrations at SMEAR II. Moreover, although many VOCs listed in Table 2, such as benzene, toluene+p-cymene, MEK, and MTs, showed higher median concentrations on SM2 days compared to the BG days, the notches mostly overlapped between the BG and SM2 days (Fig. 5). This indicates that the differences were not statistically significant for those compounds. Furthermore, it is clear that the total VOC concentrations were largely affected by winds coming from the SM1 sector.

The concentrations of acetic and formic acid did not differ statistically significantly between the sawmill sectors and the BG sector, although in Broege *et al.* (1996) differences were found in kiln-drying related emissions. Further, in Eerdekens *et al.* (2009), methanol and acetone were also related to sawmill activities, whereas in our analysis these compounds were only slightly elevated during SM1 episode days compared to the BG days, but not statistically significantly.

When dividing data seasonally, it is clear that the VOCs, which were emitted in largest quantiles by vegetation, such as MTs and isoprene+MBO, were the most influenced by the sawmills in autumn and winter (up to 7.1 times higher for MTs in SM1 compared to the BG in autumn; see Table S1 in Supplementary Information) due to the smaller background concentrations in those months (median MT concentration in winter for the BG sector was 0.021 ppb and in summer 0.137 ppb). Other VOCs showed more evenly distributed increases throughout the year, or the results between the sectors were less conclusive.

Trace and greenhouse gases

Monitored trace and greenhouse gases showed clear increases in concentration for the SM1 sector and slight increases for the SM2 sector compared to the BG sector, except O_3 that showed decreasing concentration (Fig. 6). Compounds related to anthropogenic activities, such as NO_x and SO_2, might be related to fuel consumption of machinery operation at sawmills as well as log and end-product transportation (Adhikari & Ozarska 2018) whereas the decrease in O_3 could be caused due to oxidation of elevated VOC concentrations by O_3 during sawmill episodes (Zhang *et al.* 2024). To gain better understanding of the variations in trace gas concentrations, density functions of the sector-wise divided trace gas concentrations were studied (Fig. 7). CO_2 and CH_4 concentrations

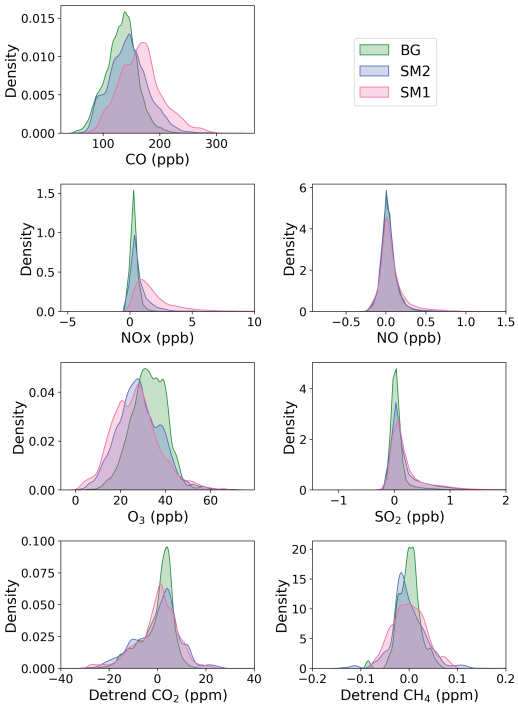

Fig 7. Density plots for the concentrations of CO, NO_x, NO, O_3, SO_2, CO_2, and CH_4 in original time resolution across wind direction sectors. CO_2 and CH_4 density plots are created after removing the linear trend.

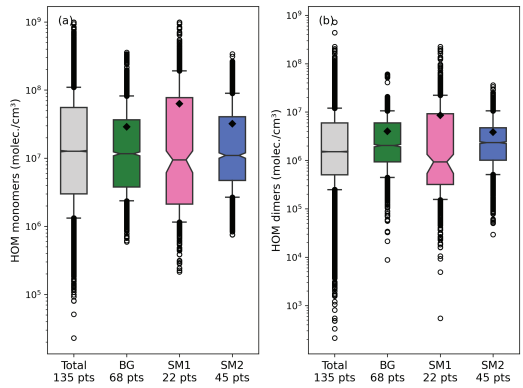

Fig 8. Boxplot of HOM (**a**) monomer and (**b**) dimer concentrations in original time resolution separated into BG, SM1, and SM2 sectors, gray marking the sum of all sectors. Markers as in Fig. 5.

were detrended since they exhibited non-stationary time series (see Fig. S3 in Supplementary Information).

In the SM1 sector, CO and NO_x were shifted towards higher concentrations and O_3 towards lower concentrations whereas other gases exhibited more similar distribution as the BG sector (Fig. 7). Again, the SM2 sector exhibited a similar shift in the distribution pattern, but its distribution overlapped more with the BG sector.

Differences in the distributions for the concentrations of NO and SO_2 were small, and a considerable number of data points fell below the detection limit of the instruments, making the analysis less reliable. The detection limits were 0.05 ppb for NO and NO_x, and 0.1 ppb for SO_2.

Distributions of detrended CO_2 and CH_4 concentrations were rather similar for all sectors, indicating that the sawmills might not cause the observed increases in concentrations for SM1 and SM2 sectors compared to the BG sector (Fig. 7), but it is likely caused by bias due to the overall increasing trend in CO_2 and CH_4 concentrations.

Polar plots of the variables (see Fig. S4 in Supplementary Information) derived from the daily median concentrations illustrate that the spatial distribution was more scattered compared to the MT plume (Fig. 2a), indicating that the trace gases have multiple sources beyond the sawmills (Riuttanen *et al.* 2013).

HOMs

To understand whether MT emissions from the sawmills could lead to production of HOMs within the travel distance to SMEAR II, we analyzed the HOM concentration distribution of all the available data from 2016 to 2023 by each wind sector (Fig. 8). For both HOM monomers and dimers, the BG and SM2 sectors did not reveal a significant difference in their distributions (similar median and IQR). On the contrary, SM1 days had a different distribution with respect to the BG sector, with a lower median and wider IQR for both HOM monomers and dimers. However, with HOM monomers the notches overlap for SM1 and BG sectors, indicating that the differences in the distributions were not statistically significant.

To investigate if we can instead find evidence of chemical reactions, leading to production of HOMs via MT oxidation (Ehn *et al.*

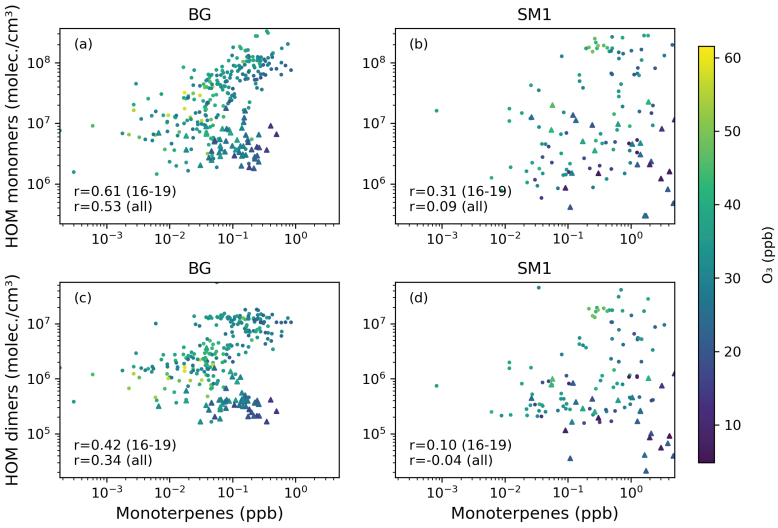

Fig 9. HOM (**a**,**b**) monomer and (**c**,**d**) dimer concentrations as a function of MT concentration colored by O_3 concentration for (**a**,**c**) the BG sector and (**b**,**d**) the SM1 sector. Dots represent the hourly median of data measured between 2016 and 2019 and triangles data measured after 2022. Correlation coefficients correspond to the 2016–2019 (16–19) data and the whole dataset (all).

2014, Bianchi *et al.* 2019), the potential correlations between HOMs, MTs, and O_3 were analyzed (Fig. 9 and Fig. S5 in Supplmentary Information). It can be noticed that the SM1 data had higher values of MTs than BG as already discovered in the VOC concentration dynamics section. In general, the BG sector shows a higher positive linear correlation between HOMs and MTs compared to the SM1 data, especially when discarding data points after the instrument maintenance in 2022, which showed more scattered values (correlation coefficient 0.61 vs. 0.31 (monomers) and 0.42 vs. 0.10 (dimers)). This might indicate that there is a lag time between the MT burst and oxidation into HOMs, or that the changes in atmospheric composition caused by the sawmill activity alter the efficiency of the chemical pathways that lead to the production of HOMs. For example, NO_x can terminate MT autoxidation to HOMs or propagate the reaction chain (Bianchi *et al.* 2019, Zhang *et al.* 2024). Furthermore, the concentrations, especially HOMs, depend on oxidation, which are affected by the level of oxidants and their oxidation capacities (Mogensen *et al.* 2015, Bianchi *et al.* 2019).

The markers in Fig. 9 clearly show the difference in HOM concentrations after the instrument maintenance conducted in 2022 as addressed in Sect. 2.4. The correlation coefficient was higher if the data available after 2022 was disregarded.

Aerosol particles

The median particle (3–1000 nm) size distributions (Fig. 10a) and the median mobility distribution of negative ions (2–10 nm) (Fig. 10b) were also investigated. Compared to the BG sector, there was an increase in particles with a diameter larger than 63 nm when the wind came from either of the two sawmill sectors. During SM1 days, there were also more particles with a diameter smaller than 10 nm compared to the BG, which was not visible during the SM2 days.

On SM1 days, there were more negative ions between 4 and 7 nm than on the BG days, and more ions with 3 nm diameter on SM2 days. There was also a peak in the ratio between SM1 days and BG days at 3 nm ions, even though the background stayed higher than for the SM1 sector. Similarly, there was also a peak in the ratio between SM2 and BG at 4.45 nm ions.

The overall lower concentration of negative ions is also visible in Fig. S6 in Supplementary Information, where the correlation between ions and the concentration of HOMs was plotted to analyze the role of HOMs in initial aerosol formation (Kulmala *et al.* 2024, Tuovinen *et al.* 2024). However, these variables showed weak positive correlation ($r = 0.2$) on SM1 days.

Clearly higher organic aerosol (OA) concentrations were observed on SM1 days compared to the background (Fig. 11), which is in

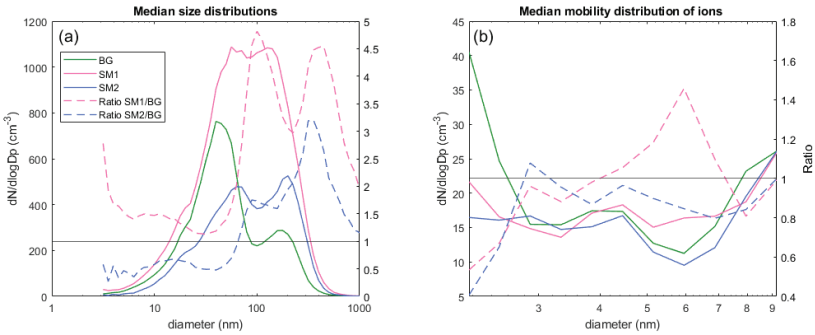

Fig 10. (**a**) Median particle size distributions and (**b**) mobility distributions of negative ions for BG, SM1, and SM2 sectors as well as ratios between sawmill and BG sectors.

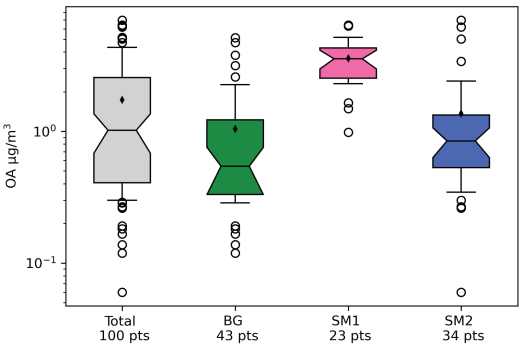

Fig 11. Boxplot of daily median organic aerosol (OA) concentration separated into BG, SM1, and SM2 sectors, gray marking the sum of all sectors. Markers as in Fig. 5.

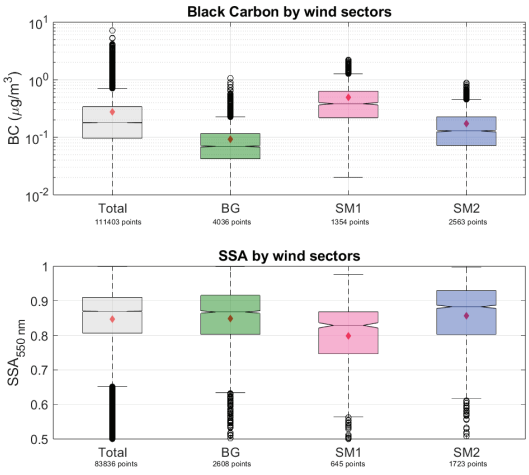

Fig 12. Boxplots of hourly averaged equivalent black carbon concentration and SSA measured at SMEAR II separated into BG, SM1, and SM2 sectors, gray marking the combination of all sectors. The median is shown with a black line, the mean value with a red diamond, and outliers with black circles. In this figure, the whiskers extend to 2.5 times the IQR range to both sides.

accordance with Heikkinen *et al.* (2020). Also, during SM2 days the median OA concentration was higher compared to the BG sector but not statistically significantly. A possible correlation between VOCs and OA was explored by evaluating the VOC/OA ratio and their relation to the concentration of O_3, temperature, and photosynthetically active radiation (PAR) (see Figs. S7 and S8 in Supplementary Information), but no clear correlations were found, and the data was too limited to draw any reliable conclusions.

Boxplots of the main aerosol optical properties, equivalent black carbon and single scattering albedo (SSA) were analyzed by wind sectors (Fig. 12). Larger concentrations of black carbon were observed on SM1 days, with a median value of 0.38 µg m^{-3} (mean 0.49 µg m^{-3}) while BG days showed very clean conditions, with a median concentration as low as 0.07 µg m^{-3} (mean 0.09 µg m^{-3}). The influence of equivalent black carbon is also visible in SSA, which varied between the different sectors, with lower values observed from the SM1 sector (median value of 0.83, against 0.87 on the BG days), which could not be explained only by the larger aerosol concentrations. This indicates that a more absorbing aerosol population reached the SMEAR II site on the SM1 days, implying that the main sources of such particles were related to human activity.

Case studies

Case studies were conducted to further analyze the dynamics of different variables during the sawmill episodes. These days include days with highest fraction of winds coming from

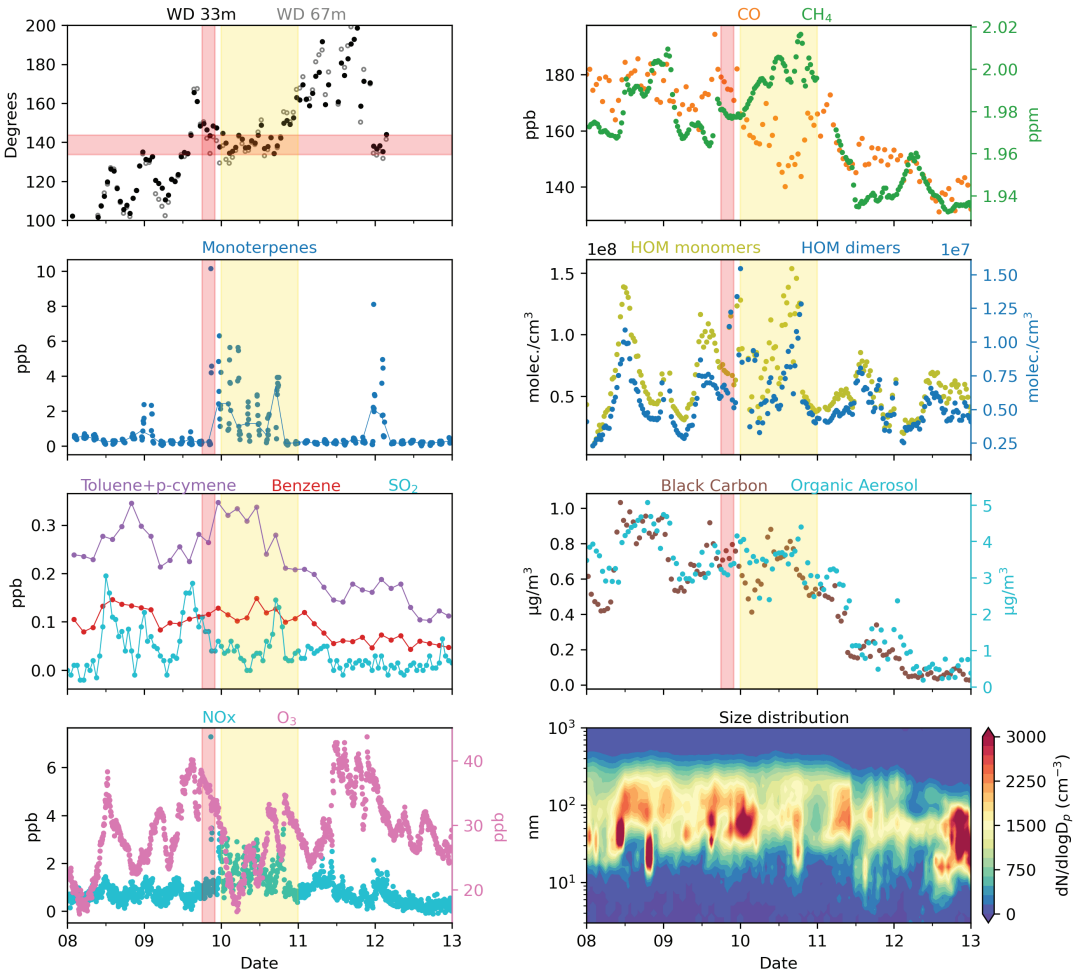

Fig 13. Case study from 8–13 Sep 2018 containing wind directions, concentrations of MTs, benzene, toluene+p-cymene, SO_2, NO_x, O_3, CO, CH_4, HOM monomers and HOM dimers, black carbon, and OA as well as particle size distribution. The day classified as sawmill episode day is indicated by the yellow shaded area, the times when air mass trajectories crossed the SM1 sector are indicated by the vertical red shaded areas, and the direction of the SM1 sector is indicated by the horizontal red shaded area. The wind directions, CO, black carbon, benzene, toluene+p-cymene, and SO_2 are one-hour medians, and the one-hour median for MTs is indicated by the blue line.

the sawmill sectors. The dates with available measurements for VOCs, trace gases, HOMs, black carbon and size distributions were manually chosen, totaling 15 days for SM1 and 9 for SM2. The time series for all measurements as well as wind direction was plotted for the two days before and after the flagged day to showcase the baseline variation. Additionally, the HYSPLIT model was used to explore the air mass origins during the same time periods. A trajectory reaching SMEAR II was considered to be influenced by SM1 or SM2 when the air mass traveled closer than 1 km to one of the sawmills within the mixed layer. Examples are given for SM1 sector on 8.–13.9.2018 (Fig. 13) and for both sectors on 5.–12.4.2019 (Fig. 14). The corresponding trajectories are shown in Figs. S9 and S10 in Supplementary Information, respectively.

The case studies showed clear SM1 sector responses for MTs, even when wind crossed the SM1 sector only briefly (Fig. 13). Similarly, the NO_x concentration increased along with the

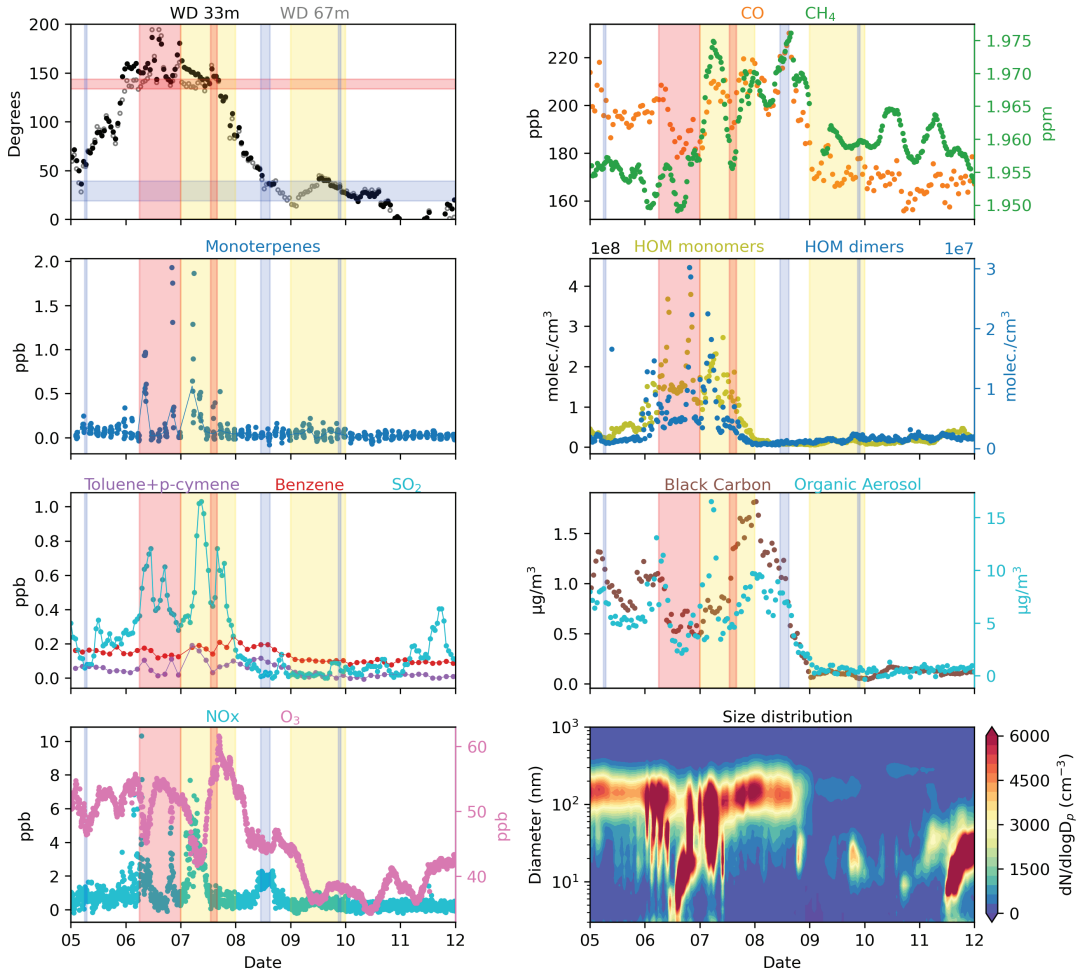

Fig 14. Case study from 5–12 April 2019 showing the same variables as in Fig. 14. The days classified as sawmill episode days are indicated by the yellow shaded areas, the times when air mass trajectories crossed the SM1 and SM2 sectors are indicated by the vertical red and blue shaded areas, and the direction of the SM1 and SM2 sectors are indicated by the horizontal red and blue shaded areas, respectively.

MTs, which is a further indication of anthropogenic activity, while the O_3 concentration correlated negatively with MTs, which could be explained by higher oxidation of VOCs (Zhang *et al.* 2024).

Rather similar trends could be seen for toluene+p-cymene and benzene, however with much weaker responses. While they both are generally markers for anthropogenic activity, the reason for toluene+p-cymene concentration following more closely the pattern of MTs could be related to increased fraction of p-cymene, which can be emitted from the wood during cutting and treatment (Granström 2009) and/or increased emissions of toluene from the sawmill activities, as it has been shown that plants release many benzenoids, including toluene, under stressed conditions (Misztal *et al.* 2015).

Although CO, CH_4, SO_2, HOMs, OA, black carbon, and aerosol size distribution showed response in concentration for the sawmill sectors (Fig. 6, 8, 10, 11, and 12), the actual connection to sawmill emissions was less clear. While on some case study days, for example, aerosol size distribution and HOM concentrations followed the trends of MTs (e.g. on 6.–7.4.2019

in Fig. 14), on other days the fluctuations were large (e.g. Fig. 13), indicating that there were also other processes affecting the concentrations, making the analysis more difficult. This was also supported by the polar plots of trace and greenhouse gases (see Fig. S4 in Supplementary Information) as the data points were by far more scattered than the monoterpene signal (Fig. 2a).

The case studies for the SM2 sector showed generally similar, yet much weaker, effects compared to the SM1 sector, making it difficult to distinguish a response from the other fluctuations (see Fig. S11 and S12 in Supplementary Information). Maximum increases in MT concentrations remained mostly below 0.3 ppb along with small increases in NO_x concentration.

A time period was identified where SM1 and SM2 episodes occurred with only one day in between (Fig. 14). Here, the differences between the two sawmills are clear, with significant increases in the MTs (around 2 ppb), during the SM1 day while only a slight deviation from the baseline, up to 0.25 ppb, can be seen for the SM2 day. Additionally, increases in toluene+p-cymene and HOMs coincided with the increases in MTs during SM1 episode. Lastly, the air mass trajectories were also investigated as a marker for SM2 influenced air masses due to the longer distance to SMEAR II. Indeed, it can be seen that while the trace and greenhouse gases did not show clear effects during the SM2 day flagged by the wind direction, they responded during the air mass trajectory flagged on 8.4.2019, which was especially clear with NO_x.

Examination of air mass back trajectories also revealed that during most of the cases when winds crossed the SM1 sector they traveled through urban and industrial areas in Russia and eastern Europe, which are known to be sources of anthropogenic pollutants measured at SMEAR II (Riuttanen *et al.* 2013). Hence, the observed fluctuations in analyzed parameters beside sawmill episodes could be related to these long-range transported pollutants. Moreover, similar air mass source areas were detected during SM2 episodes (see Fig. S10 in Supplementary Information), which could also explain why clearer trace gas responses coincide with air mass trajectories from the SM2 direction.

Conclusions and summary

This study utilized long-term (2011–2023) field data to identify and quantify the effects of close-by sawmills on the concentrations of various compounds, measured over a boreal forest. The sawmills affected most importantly MTs, NO_x, O_3, and mainly Aitken mode sized aerosol particles, and the effects were especially clear for the days classified as influenced by the Korkeakoski sawmills (SM1 sector), whereas the effect of Vilppula sawmill (SM2 sector), located further away, was minor. The comprehensive, long-term observations at SMEAR II and the clear emission source gave us tools to analyze atmospheric chemistry and aerosol processes in the point of view of their emissions and sinks.

The sawmill episodes were classified by wind direction whereas in previous studies the analysis was based on the extremes observed in monoterpene concentrations (Liao *et al.* 2011) and formation of new particles during nighttime (Eerdekens *et al.* 2009). The new approach enabled us to analyze all simultaneous impacts, regardless of their magnitude. By analyzing multiple parameters, we noticed that the signal from the sawmills in Korkeakoski (SM1 sector) was clearly captured using only 10° (133.7°–143.7°) wind sector, while Liao *et al.* (2011) suggested using a larger, 20° sector (120°–140°).

The clearest response was seen in MT concentration, which was expected, since boreal coniferous trees naturally produce MTs, which are then released at sawmills in cutting and drying processes of the wood (Ingram *et al.* 1995, Granström 2007). Although the sawmill activities from the SM1 direction were visible in all seasons, the effect was particularly distinct from autumn to spring, both because of lower biogenic MT emissions from the forest and higher number of SM1 episode days. The impact of the SM2 episodes was much smaller, likely due to longer travel distance and the wind direction from the SM2 being rather rare, even though they were more evenly distributed throughout the year. Hence, the influence of sawmill related emissions on ecosystem–atmosphere studies, focusing mainly on growing season, is less critical, although highly advisable to take into account in future studies. For other trace

gases and aerosol particles, unambiguous separation between sawmill related emissions and long-range transported pollution proved to be challenging as the compounds from different sources are mixed in the atmosphere.

Acknowledgements: The work was supported by ACCC Flagship funded by the Research Council of Finland (grant number 357902, 359340). We acknowledge the technical and scientific staff maintaining measurements at SMEAR II, including Dr. Pasi P. Aalto (DMPS measurements), Dr. Janne Lampilahti (NAIS measurements), Dr. Frans Graeffe (ACSM measurements), and Dr. Petri Keronen (trace gas measurements). We thank ACTRIS for aerosol and condensable vapors and ICOS for CH_4 and CO_2 measurements at SMEAR II. Finally, we are sincerely grateful for Prof. Tuukka Petäjä and Prof. Jaana Bäck for their efforts to sustain long-term measurements at the SMEAR II station.

Supplementary Information: The supplementary information related to this article is available online at: https://doi.org/10.60910/ber2025.727e-sw95

References

Aalto, J., Porcar-Castell, A., Atherton, J., Kolari, P., Pohja, T., Hari, P., Nikinmaa, E., Petäjä, T. & Bäck, J. 2015. Onset of photosynthesis in spring speeds up monoterpene synthesis and leads to emission bursts. *Plant, cell & environment* 38(11): 2299–2312, https://doi.org/10.1111/pce.12550.

Aalto, P., Hämeri, K., Becker, E., Weber, R., Salm, J., Mäkelä, J. M., Hoell, C., O'dowd, C. D., Hansson, H.-C., Väkevä, M., Koponen, I., Buzorius, G. & Kulmala, M. 2001. Physical characterization of aerosol particles during nucleation events. *Tellus B: Chemical and Physical Meteorology* 53(4):344–358.

Adhikari, S. & Ozarska, B. 2018. Minimizing environmental impacts of timber products through the production process "From Sawmill to Final Products". *Environ Syst Res* 7, https://doi.org/10.1186/s40068-018-0109-x.

Artaxo, P., Hansson, H.-C., Andreae, M.O., Bäck, J., Alves, E.G., Barbosa, H.M.J., Bender, F., Bourtsoukidis, E., Carbone, S., Chi, J., Decesari, S., Després, V.R., Ditas, F., Ezhova, E., Fuzzi, S., Hasselquist, N.J., Heintzenberg, J., Holanda, B.A., Guenther, A., Hakola, H., Heikkinen, L., Kerminen, V.-M., Kontkanen, J., Krejci, R., Kulmala, M., Lavric, J.V., de Leeuw, G., Lehtipalo, K., Machado, L.A.T., McFiggans, G., Franco, M.A.M., Meller, B.B., Morais, F.G., Mohr, C., Morgan, W., Nilsson, M.B., Peichl, M., Petäjä, T., Praß, M., Pöhlker, C., Pöhlker, M.L., Pöschl, U., Von Randow, C., Riipinen, I., Rinne, J., Rizzo, L.V., Rosenfeld, D., Silva Dias, M.A.F., Sogacheva, L., Stier, P., Swietlicki, E., Sörgel, M., Tunved, P., Virkkula, A., Wang, J., Weber, B., Yáñez-Serrano, A.M., Zieger, P., Mikhailov, E., Smith, J.N. & Kesselmeier, J. 2022. Tropical and Boreal Forest – Atmosphere Interactions: A Review. *Tellus B: Chemical and Physical Meteorology* 74(1): 24–163, https://doi.org/10.16993/tellusb.34.

Aslan, T., Launiainen, S., Kolari, P., Peltola, O., Aalto, J., Bäck, J., Vesala, T. & Mammarella, I. 2024. Thinning turned boreal forest to a temporary carbon source - short term effects of partial harvest on carbon dioxide and water vapor fluxes. *Agricultural and Forest Meteorology* 353: 110061.

Bianchi, F., Kurtén, T., Riva, M., Mohr, C., Rissanen, M. P., Roldin, P., Berndt, T., Crounse, J. D., Wennberg, P. O., Mentel, T. F., Wildt, J., Junninen, H., Jokinen, T., Kulmala, M., Worsnop, D. R., Thornton, J. A., Donahue, N., Kjaergaard, H. G. & Ehn, M. 2019. Highly Oxygenated Organic Molecules (HOM) from Gas-Phase Autoxidation Involving Peroxy Radicals: A Key Contributor to Atmospheric Aerosol. *Chemical Reviews* 119 (6): 3472-3509, DOI: 10.1021/acs.chemrev.8b00395.

Broege, K., Aehlig, K. & Scheithauer, M. 1996. Emissionen aus schnittholztrocknern. Institut fur Holztechnologie Dresden.

Bäck, J., Aalto, J., Henriksson, M., Hakola, H., He, Q. & Boy, M. 2012. Chemodiversity of a Scots pine stand and implications for terpene air concentrations. *Biogeosciences* 9: 689–702, https://doi.org/10.5194/bg-9-689-2012.

Dal Maso, M., Kulmala, M., Riipinen, I., Wagner, R., Hussein, T., Aalto, P. P. & Lehtinen, K. E. 2005. Formation and growth of fresh atmospheric aerosols: eight years of aerosol size distribution data from SMEAR II, Hyytiälä, Finland. *Boreal Environment Research* 10(5): 323-336.

Drinovec, L., Močnik, G., Zotter, P., Prévôt, A. S. H., Ruckstuhl, C., Coz, E., Rupakheti, M., Sciare, J., Müller, T., Wiedensohler, A., and Hansen, A. D. A. 2015. The "dual-spot" Aethalometer: an improved measurement of aerosol black carbon with real-time loading compensation, *Atmos. Meas. Tech*., 8: 1965–1979, https://doi.org/10.5194/amt-8-1965-2015.

Eerdekens, G., Yassaa, N., Sinha, V., Aalto, P. P., Aufmhoff, H., Arnold, F., Fiedler, V., Kulmala, M. & Williams, J. 2009. VOC measurements within a boreal forest during spring 2005: on the occurrence of elevated monoterpene concentrations during night time intense particle concentration events. *Atmos. Chem. Phys*. 9: 8331–8350, https://doi.org/10.5194/acp-9-8331-2009.

Ehn, M., Thornton, J.A., Kleist, E., Sipilä, M., Junninen, H., Pullinen, I., Springer, M., Rubach, F., Tillmann, R., Lee, B., Lopez-Hilfiker, F., Andres, S., Acir, I.-H., Rissanen, M., Jokinen, T., Schobesberger, S., Kangasluoma, J., Kontkanen, J., Nieminen, T., Kurtén, T., Nielsen, L.B., Jørgensen, S., Kjaergaard, H.G., Canagaratna, M., Dal Maso, M., Berndt, T., Petäjä, T., Wahner, A., Kerminen, V.-M., Kulmala, M., Worsnop, D.R., Wildt, J. & Mentel, T.F., 2014. A large source of low-volatility secondary organic aerosol. *Nature* 506: 476–479, https://doi.org/doi:10.1038/nature13032.

Englund, F. & Nussbaum, R. M. 2000. Monoterpenes in scots pine and norway spruce and their emission during kiln drying. Holzforschung 54(5):449–456.

Ghirardo, A., Koch, K., Taipale, R., Zimmer, I., Schnitzler, J.-P. & Rinne, J. 2010. Determination of de novo and pool emissions of terpenes from four common boreal/alpine trees by 13CO2 labelling and PTR-MS analysis. *Plant, Cell & Environment* 33(5):781–792.

Granström, K. M. 2007. Wood processing as a source of terpene emissions compared to natural sources. *Air Pollution XV*. 1: 263-272.

Granström, K. M. 2009. Underestimation of Terpene Exposure in the Nordic Wood Industry. Journal of Occupational and Environmental Hygiene 7(3): 144–151, https://doi.org/10.1080/15459620903476330.

Gregow, H., Rantanen, M., Laurila, T. K. & Mäkelä, A. 2020. Review on winds, extratropical cyclones and their impacts in northern Europe and Finland. *Finnish Meteorological Institute*.

Grote R. & Niinemets Ü. 2008. Modeling volatile isoprenoid emissions – a story with split ends. *Plant Biology* 10: 8–28.

Haapanala, S., Hakola, H., Hellén, H., Vestenius, M., Levula, J. & Rinne, J. 2012. Is forest management a significant source of monoterpenes into the boreal atmosphere? *Biogeosciences* 9(4): 1291–1300.

Hakola, H., Hellén, H., Hemmilä, M., Rinne, J. & Kulmala, M. 2012 In situ measurements of volatile organic compounds in a boreal forest. *Atmos. Chem. Phys*. 12: 11665–11678, https://doi.org/10.5194/acp-12-11665-2012.

Hari, P. & Kulmala, M. 2005. Station for measuring ecosystem-atmosphere relations (SMEAR II). *Boreal Environment Research* 10(5): 315–322.

Heikkinen, L., Äijälä, M., Riva, M., Luoma, K., Dällenbach, K., Aalto, J., Aalto, P., Aliaga, D., Aurela, M., Keskinen, H., Makkonen, U., Rantala, P., Kulmala, M., Petäjä, T., Worsnop, D. & Ehn, M. 2020. Long-term sub-micrometer aerosol chemical composition in the boreal forest: inter- and intra-annual variability. *Atmospheric Chemistry and Physics* 20(5): 3151–3180.

Hellén, H., Hakola, H., Reissell, A. & Ruuskanen, T. 2004. Carbonyl compounds in boreal coniferous forest air in hyytiälä, southern Finland. *Atmospheric chemistry and physics* 4(7): 1771–1780.

Hellén, H., Praplan, A. P., Tykkä, T., Ylivinkka, I., Vakkari, V., Bäck, J., Petäjä, T., Kulmala, M. & Hakola, H. 2018. Long-term measurements of volatile organic compounds highlight the importance of sesquiterpenes for the atmospheric chemistry of a boreal forest. *Atmos. Chem. Phys*. 18: 13839–13863, https://doi.org/10.5194/acp-18-13839-2018.

Hyvärinen, A.-P., Kolmonen, P., Kerminen, V.-M., Virkkula, A., Leskinen, A., Komppula, M., Hatakka, J., Burkhart, J., Stohl, A., Aalto, P., Kulmala, M., Lehtinen, K., Viisanen, Y. & Lihavainen, H. 2011. Aerosol black carbon at five background measurement sites over Finland, a gateway to the arctic. *Atmospheric Environmen*t 45(24): 4042–4050.

Ingram, L., Taylor, F., Punsavon, V. & Templeton, M. 1995. Identification of volatile organic compounds emitted during drying of southern pine in pilot and laboratory experiments. In Measuring and Controlling VOC and Particulate Emissions from Wood Processing Operations and Wood Based Products. *Forest Products Society*, Madison WI, pp. 35-40.

Jokinen, T., Sipilä, M., Junninen, H., Ehn, M., Lönn, G., Hakala, J., Petäjä, T., Mauldin III, R. L., Kulmala, M. & Worsnop, D. R. 2012. Atmospheric sulphuric acid and neutral cluster measurements using ci-api-tof. Atmospheric *Chemistry and Physics* 12(9): 4117–4125.

JPJ 2025. JPJ-Wood sawmill. https://jpj-wood.fi/en/company. Accessed: 19.09.2025.

Kansal, A. 2009. Sources and reactivity of NMHCs and VOCs in the atmosphere: A review. *Journal of Hazardous Materials* 166(1): 17–26, https://doi.org/10.1016/j.jhazmat.2008.11.048.

Kerminen, V.-M., Paramonov, M., Anttila, T., Riipinen, I., Fountoukis, C., Korhonen, H., Asmi, E., Laakso, L., Lihavainen, H., Swietlicki, E., Svenningsson, B., Asmi, A., Pandis, S. N., Kulmala, M. & Petäjä, T. 2012. Cloud condensation nuclei production associated with atmospheric nucleation: a synthesis based on existing literature and new results. *Atmospheric Chemistry and Physics* 12(24): 12037–12059.

Kulmala, M., Ke, P., Lintunen, A., Peräkylä, O., Lohtander, A., Tuovinen, S., Lampilahti, J., Kolari, P., Schiestl-Aalto, P., Kokkonen, T., Nieminen, T., Dada, L., Ylivinkka, I., Petäjä, T., Bäck, J., Lohila, A., Heimsch, L., Ezhova, E. & Kerminen, V.-M. 2024. A novel concept for assessing the potential of different boreal ecosystems to mitigate climate change (carbonsink+ potential). *Boreal Environment Research* 29: 1–16.

Lampilahti, J., Manninen, H. E., Nieminen, T., Mirme, S., Ehn, M., Pullinen, I., Leino, K., Schobesberger, S., Kangasluoma, J., Kontkanen, J., Järvinen, E., Väänänen, R., Yli-Juuti, T., Krejci, R., Lehtipalo, K., Levula, J., Mirme, A., Decesari, S., Tillmann, R., Worsnop, D. R., Rohrer, F., Kiendler-Scharr, A., Petäjä, T., Kerminen, V.-M., Mentel, T. F. & Kulmala, M. 2021. Zeppelin-led study on the onset of new particle formation in the planetary boundary layer, *Atmos. Chem. Phys*., 21: 12649–12663, https://doi.org/10.5194/acp-21-12649-2021.

Liao, L., Dal Maso, M., Taipale, R., Rinne, J., Ehn, M., Junninen, H., Aijala, M., Nieminen, T., Alekseychik, P., Hulkkonen, M., Worsnop, D., Kerminen, V.-M. & Kulmala, M. 2011. Monoterpene pollution episodes in a forest environment: Indication of anthropogenic origin and association with aerosol particles. *Boreal Environment Research* 16: 288–303.

Liebmann, J., Karu, E., Sobanski, N., Schuladen, J., Ehn, M., Schallhart, S., Quéléver, L., Hellen, H., Hakola, H., Hoffmann, T., Williams, J., Fischer, H., Lelieveld, J. & Crowley, J. N. 2018. Direct measurement of NO_3 radical reactivity in a boreal forest. *Atmos. Chem. Phys*. 18: 3799–3815, https://doi.org/10.5194/acp-18-3799-2018.

Luoma, K., Virkkula, A., Aalto, P., Lehtipalo, K., Petäjä, T. & Kulmala, M. 2021. Effects of different correction algorithms on absorption coefficient – a comparison of three optical absorption photometers at a boreal forest site. *Atmos. Meas. Tech*. 14: 6419–6441, https://doi.org/10.5194/amt-14-6419-2021.

Metsä Group 2024. Metsä Group Vilppula sawmill. https://

www.metsagroup.com/metsafibre/about-metsafibre/sawn-timber-production/vilppula-sawmill/. Accessed: 19.09.2025.

Mirme, S. & Mirme, A. 2013. The mathematical principles and design of the NAIS – a spectrometer for the measurement of cluster ion and nanometer aerosol size distributions, *Atmos. Meas. Tech*., 6: 1061–1071, https://doi.org/10.5194/amt-6-1061-2013.

Misztal, P.K., Hewitt, C.N., Wildt, J., Blande, J.D., Eller, A.S.D., Fares, S., Gentner, D.R., Gilman, J.B., Graus, M., Greenberg, J., Guenther, A.B., Hansel, A., Harley, P., Huang, M., Jardine, K., Karl, T., Kaser, L., Keutsch, F.N., Kiendler-Scharr, A., Kleist, E., Lerner, B.M., Li, T., Mak, J., Nölscher, A.C., Schnitzhofer, R., Sinha, V., Thornton, B., Warneke, C., Wegener, F., Werner, C., Williams, J., Worton, D.R., Yassaa, N. & Goldstein, A.H. 2015. Atmospheric benzenoid emissions from plants rival those from fossil fuels. *Scientific Reports* 5: 12064, https://doi.org/10.1038/srep12064.

Mogensen, D., Gierens, R., Crowley, J.N., Keronen, P., Smolander, S., Sogachev, A., Nölscher, A.C., Zhou, L., Kulmala, M., Tang, M.J., Williams, J. & Boy, M. 2015. Simulations of atmospheric OH, O_3 and NO_3 reactivities within and above the boreal forest. *Atmospheric Chemistry and Physics* 15: 3909–3932, https://doi.org/10.5194/acp-15-3909-2015.

Mohr, C., Thornton, J.A., Heitto, A. Lopez-Hilfiker, F. D., Lutz, A., Riipinen, I., Hong, J., Donahue, N. M., Hallquist, M., Petäjä, T., Kulmala, M. & Yli-Juuti, T. 2019. Molecular identification of organic vapors driving atmospheric nanoparticle growth. *Nat Commun* 10: 4442, https://doi.org/10.1038/s41467-019-12473-2.

Neefjes I., Laapas M., Liu Y., Médus E., Miettunen E., Ahonen L., Quéléver L., Aalto J., Bäck J., Kerminen V-M., Lamplahti J., Luoma K., Mäki M., Mammarella I., Petäjä T., Räty M., Sarnela N., Ylivinkka I., Hakala S., Kulmala M., Nieminen T. & Lintunen A. 2022. 25 years of atmospheric and ecosystem measurements in a boreal forest — Seasonal variation and responses to warm and dry years. *Boreal Env. Res*. 27: 1–31.

Neimane-Šroma, S., Durand, M., Lintunen, A., Aalto, J., and Robson, T. M. 2024. Shedding light on the increased carbon uptake by a boreal forest under diffuse solar radiation across multiple scales. *Global Change Biology* 30: e17275, https://doi.org/10.1111/gcb.17275.

Peräkylä, O., Vogt, M., Tikkanen, O., Laurila, T., Kajos, M., Rantala, P., Patokoski, J., Aalto, J., Yli-Juuti, T., Ehn, M., Sipilä, M., Paasonen, P., Rissanen, M., Nieminen, T., Taipale, R., Keronen, P., Lappalainen, H. K., Ruuskanen, T. M., Rinne, J., Kerminen, V.-M., Kulmala, M., Bäck, J. & Petäjä, T. 2014. Monoterpenes' oxidation capacity and rate over a boreal forest: temporal variation and connection to growth of newly formed particles. *Boreal Environment Research* 19(Suppl. B):293–310.

Rannik, Ü., Keronen, P., Hari, P., and Vesala, T. 2004. Estimation of forest–atmosphere co2 exchange by eddy covariance and profile techniques. *Agricultural and Forest Meteorology* 126(1):141–155.

Rinne, J., Back, J., and Hakola, H. 2009. Biogenic volatile organic compound emissions from the eurasian taiga: Current knowledge and future directions. Boreal Environment Research 14: 807–826.

Riuttanen, L., Hulkkonen, M., Dal Maso, M., Junninen, H. & Kulmala, M. 2013. Trajectory analysis of atmospheric transport of fine particles, SO2, NOx and O3 to the smear ii station in Finland in 1996-2008. *Atmospheric Chemistry and Physics* 13(4): 2153–2164.

Räisänen, T., Ryyppö, A. & Kellomäki, S. 2008. Impact of timber felling on the ambient monoterpene concentration of a Scots pine (Pinus sylvestris l.) forest. Atmospheric Environment 42(28): 6759–6766.

Seinfeld, J. H. & Pandis, S. N. 2012. Atmospheric Chemistry and Physics: From Air Pollution to Climate Change. John Wiley & Sons, Washington, United States of America.

Sinclair, V. A., Ritvanen, J., Urbancic, G., Erner, I., Batrak, Y., Moisseev, D. & Kurppa, M. 2022. Boundary-layer height and surface stability at Hyytiälä, Finland, in ERA5 and observations, *Atmos. Meas. Tech*., 15: 3075–3103, https://doi.org/10.5194/amt-15-3075-2022.

Snoun, H., Krichen, M. & Chérif, H. 2023. A comprehensive review of Gaussian atmospheric dispersion models: current usage and future perspectives. *Euro-Mediterranean Journal for Environmental Integration*, 8(1): 219-242.

Stein, A. F., Draxler, R. R., Rolph, G. D., Stunder, B. J. B., Cohen, M. D. & Ngan, F. 2015. NOAA's hysplit atmospheric transport and dispersion modeling system. *Bulletin of the American Meteorological Society* 96(12): 2059 – 2077.

Straumfors, A., Corbin, M., McLean, D., 't Mannetje, A., Olsen, R., Afanou, A., Daae, H.-L., Skare, Ø., Ulvestad, B., Johnsen, W. E. & Douwes, J. 2020. Exposure determinants of wood dust, microbial components, resin acids and terpenes in the saw-and planer mill industry. *Annals of work exposures and health* 64(3): 282-296.

Taipale, R., Ruuskanen, T. M., Rinne, J., Kajos, M. K., Hakola, H., Pohja, T. & Kulmala, M. 2008. Technical Note: Quantitative long-term measurements of VOC concentrations by PTR-MS — measurement, calibration, and volume mixing ratio calculation methods. *Atmospheric Chemistry and Physics* 8(22): 6681–6698.

Tunved, P., Hansson, H.-C., Kerminen, V.-M., Ström, J., Dal Maso, M., Lihavainen, H., Viisanen, Y., Aalto, P. P., Komppula, M., and Kulmala, M. 2006. High Natural Aerosol Loading over Boreal Forests. *Science* 312(5771): 261–263.

Tuovinen, S., Lampilahti, J., Kerminen, V.-M. & Kulmala, M. 2024. Intermediate ions as indicator for local new particle formation. *Aerosol Research* 2(1): 93–105.

UNECE 2010. United Nations Economic Commission for Europe/Food and Agriculture Organization of the United Nations, Timber Section, Geneva, Switzerland. 2010. Forest product conversion factors for the UNECE region, ISSN 1020 7228, https://unece.org/DAM/timber/publications/DP-49.pdf.

UPM 2016. UPM Timber Korkeakoski Brochure. https://www.upmtimber.com/siteassets/documents/brochures/upm_timber_korkeakoski_6-sesite_en.pdf. In Finnish.

Accessed: 19.09.2025.

UPM 2025a. UPM Timber Korkeakoski Sawmill. https://www.upmtimber.com/about-us/production-units/upm-korkeakoski-sawmill/. Accessed: 19.09.2025.

Virkkula, A., Mäkelä, T., Hillamo, R., Yli-Tuomi, T., Hirsikko, A., Hämeri, K. & Koponen, I. K. 2007. A simple procedure for correcting loading effects of Aethalometer data. *J. Air Waste Ma*. 57: 1214–1222, https://doi.org/10.3155/1047-3289.57.10.1214.

Wallace, J. M. & Hobbs, P. V. 2006. Atmospheric science: an introductory survey, Atmospheric science, 2nd edition, Academic Press.

Williams, J., Crowley, J., Fischer, H., Harder, H., Martinez, M., Petäjä, T., Rinne, J., Bäck, J., Boy, M., Dal Maso, M., Hakala, J., Kajos, M., Keronen, P., Rantala, P., Aalto, J., Aaltonen, H., Paatero, J., Vesala, T., Hakola, H., Levula, J., Pohja, T., Herrmann, F., Auld, J., Mesarchaki, E., Song, W., Yassaa, N., Nölscher, A., Johnson, A. M., Custer, T., Sinha, V., Thieser, J., Pouvesle, N., Taraborrelli, D., Tang, M. J., Bozem, H., Hosaynali-Beygi, Z., Axinte, R., Oswald, R., Novelli, A., Kubistin, D., Hens, K., Javed, U., Trawny, K., Breitenberger, C., Hidalgo, P. J., Ebben, C. J., Geiger, F. M., Corrigan, A. L., Russell, L. M., Ouwersloot, H. G., Vilà-Guerau de Arellano, J., Ganzeveld, L., Vogel, A., Beck, M., Bayerle, A., Kampf, C. J., Bertelmann, M., Köllner, F., Hoffmann, T., Valverde, J., González, D., Riekkola, M.-L., Kulmala, M. & Lelieveld, J. 2011. The summertime Boreal forest field measurement intensive (HUMPPA-COPEC-2010): an overview of meteorological and chemical influences. *Atmos. Chem. Phys*. 11: 10599–10618, https://doi.org/10.5194/acp-11-10599-2011.

Yli-Juuti, T., Mielonen, T., Heikkinen, L., Arola, A., Ehn, M., Isokääntä, S., Keskinen, H.-M., Kulmala, M., Laakso, A., Lipponen, A., Luoma, K., Mikkonen, S., Nieminen, T., Paasonen, P., Petäjä, T., Romakkaniemi, S., Tonttila, J., Kokkola, H. & Virtanen, A. 2021. Significance of the organic aerosol driven climate feedback in the boreal area. *Nature Communications* 12(1): 1–9.

Zhang, J., Zhao, J., Wollesen de Jonge, R., Sarnela, N., Roldin, P. & Ehn, M. 2024. Evaluating the Applicability of a Real-Time Highly Oxygenated Organic Molecule (HOM)-Based Indicator for Ozone Formation Sensitivity at a Boreal Forest Station. *Environmental Science & Technology Letters* 11(11): 1227-1232, DOI: 10.1021/acs.estlett.4c00733.

Zha, Q., Yan, C., Junninen, H., Riva, M., Sarnela, N., Aalto, J., Quéléver, L., Schallhart, S., Dada, L., Heikkinen, L., Peräkylä, O., Zou, J., Rose, C., Wang, Y., Mammarella, I., Katul, G., Vesala, T., Worsnop, D. R., Kulmala, M., Petäjä, T., Bianchi, F. & Ehn, M. 2018. Vertical characterization of highly oxygenated molecules (HOMs) below and above a boreal forest canopy, *Atmos. Chem. Phys.*, 18: 17437–17450, https://doi.org/10.5194/acp-18-17437-2018.